Different Concepts of Grid-Connected Microgrids with a PV System, Battery Energy Storage, Feed-in Tariff, and Load Management Using Fuzzy Logic

Lena ZEC, Jovan MIKULOVIC
University of Belgrade, Faculty of Electrical Engineering, Belgrade, 11000, Serbia
zl165003p@student.etf.bg.ac.rs

***Abstract*—This paper presents different variants of smart grid-connected microgrids consisting of a photovoltaic (PV) system and batteries. Based on ten-minute data on the consumption of the distribution system, the estimation of the consumption diagram of one household was performed, as well as the determination of its unmanageable and manageable part. The fuzzy logic controller and algorithm for energy flow management were applied to manage the consumption of one household. The proposed load management provides a continuous power supply to a consumer from his PV system, batteries, and distribution grid, enabling the energy exchange with the grid and achieving financial gain. The input data for the fuzzy logic controller are the difference between the PV system power production and the household power consumption, the variation of the price of electricity on the market to its average value, and the state of charge of the battery. The output data from the fuzzy logic controller are the probabilities of engaging home appliances. The presented analysis was done for a period of one year for the city of Belgrade.**

***Index Terms*—batteries, fuzzy logic, load management, microgrids, photovoltaic systems.**

I. INTRODUCTION

Increased needs for environmental protection, as well as growing problems related to the world's energy deficit, encourage investments in the field of renewable energy resources (RES). The agreement on climate in Paris from December 2017 aims to reduce greenhouse gas emissions by 47% by 2030 and achieve a neutral balance of carbon dioxide (CO2) emissions by 2070. This agreement should limit the increase in the average global temperature on the earth's surface below 2 °C (maximum 1.7 °C) by the end of this century compared to the period before the Industrial Revolution. To achieve this goal, nowadays there is a high trend of building the capacity of RES, especially solar and wind power plants. In addition to large systems connected to the electricity system, small on-grid and off-grid systems, i.e. so-called microgrids have a significant share in the installed capacities of renewable energy sources.

The microgrid implies a controllable group of consumers and producers of relatively small installed powers such as solar power plants and wind turbines, fuel cells, and energy storage systems. The microgrid can be off-grid (islanded) or connected to the distribution grid. Microgrids are suitable for improving the reliability and resilience of distribution grids and integrating the distributed renewable energy sources [1]. In case when the microgrid is connected to the distribution grid, the distribution grid becomes active. An active distribution grid is more reliable in terms of power supply to consumers, which is an advantage in case of large disturbances in the transmission grid. The reliability of consumer supply increases with the increasing number of energy sources in the distribution grid, especially if there are energy storage systems. The presence of energy sources in the distribution grid can have a favorable effect on the reduction of congestion in the distribution grid, on the reduction of electricity flows from the transmission grid to the distribution grid, as well as on the reduction of electricity transmission losses.

The efficiency of the microgrid increases if there is a possibility of managing the flow of electricity between sources, loads, and energy storage systems, especially if there is a possibility of load management. Many authors have dealt with algorithms and optimization methods to increase efficiency by combining different renewable energy sources and storage systems in the distribution grid. Papers [2-4] presented overviews of different methods, solutions, and technologies used to achieve optimal operation, energy scheduling, and system reliability in both off-grid and grid-connected types of microgrids. Paper [5] presents an overview of genetic algorithms, fuzzy logic, particle swarm optimization, and other power flow optimization techniques applied to hybrid systems. In [6], an on-grid PV/Wind hybrid system was modeled and optimized using the PSO Fuzzy algorithm. In [7], the authors have introduced a new Fuzzy Logic - Grey Wolf Optimization (FL-GWO) expert system for the grid-connected microgrid based on an intelligent meta-heuristic method for battery sizing. The fuzzy logic power management system presented in [8] enables real-time utilization of solar and wind resources in the most efficient way, thus ensuring continuous power supply. Paper [9] considered the off-grid PV-wind-battery system, while the paper [10] considered the on-grid microgrid, both using Fuzzy Logic Controller (FLC) to provide a balance between production and consumption, maintaining the battery state of charge within the permitted limits. It is also important when using the microgrid to provide appropriate power quality, i.e. to take into account

The authors are grateful to the Ministry of Science and Technological Development of Serbia for the support of this work through technological project III42009 and TR-33037.

Digital Object Identifier 10.4316/AECE.2022.03004

the value of voltage, frequency, as well as the power factor control. In [11], the authors dealt with the primary frequency control of a microgrid with a wind turbine using an FLC that controls the wind turbine pitch angle. The authors of [12] studied the harmonic impact of a distribution generator in a microgrid. Paper [13] proposes conservative power theory and control techniques for harmonic and reactive compensators oriented to smart micro-grids, where supply voltage distortion and frequency variation can be non-negligible.

From the economic point of view, the higher the efficiency of the microgrid, the more cost-effective it is. In [14], an optimal algorithm is proposed to minimize electricity consumption in accordance with tariffs as the objective from the user perspective and to minimize the power demand from the energy supplier perspective considering the characteristics of the appliances and human behavior pattern. Energy produced from PV systems can be stored in batteries and then used during the period with the high energy consumption to supply the loads in the distribution grid. The Fuzzy logic controller given in [15] can adjust FLC parameters while minimizing the number of fuzzy rules. The main goal was to manage the power flow in the microgrid model and maximize the economic return when the microgrid is equipped with an energy storage system. In the paper [16], using genetic algorithms, the day-ahead microgrid scheduling is achieved using a fuzzy expert system for controlling the power output of the storage system according to load demand, wind power availability, and electricity prices. The study [17] uses intelligent energy management for a microgrid and fuzzy logic expert system for battery scheduling while minimizing costs and greenhouse gas emissions. The paper [18] presents a residential grid-connected microgrid that uses low complexity FLC to minimize fluctuations and power peaks in the power profile exchanged with the grid while keeping the energy stored in the battery between secure limits. In [19], the logic-based energy management system aims to reduce the average peak load and operating costs through the arbitration operation of the energy storage system. In [20], the optimized FLC was adopted as a decision-making module for power flow management in the microgrid supported by a battery energy storage system used to improve the tasks of energy trading with the main grid. The paper [21] presents an intelligent economic strategy for smart grids based on fuzzy logic to minimize the grid power profile fluctuations since the renewable generation and the load demand were considered uncontrollable. Paper [22] deals with optimal energy dispatch strategies for grid-connected wind turbines with the battery energy storage system to maximize operating profit. Efficient power management and sizing of an off-grid PV-wind system with energy storage is presented in [23]. The results achieved by applying the power flow control algorithm reduced the investment costs of batteries by 33% and slightly reduced consumption by 1.35%. Significantly better results were achieved by using the fuzzy logic controller, which reduced the number of batteries by 50% and reduced energy consumption by 4.9%, while user comfort was not significantly impaired. In [24], an approximate dynamic programming algorithm is proposed to maximize the profit generated by the sale of over-generated renewable energy and minimize costs to meet the load demand in the microgrid. In [25], three optimization models and the coordination strategy for diversified community power consumers are proposed with the microgrid operation constraints: electricity bill minimization, green consumption and power reliability.

This paper presents a methodology for efficient power flow control and load management in the microgrid with a PV system as an energy source to achieve a financial gain in energy exchange with the distribution grid. Different microgrid concepts with and without energy storage, with and without feed-in tariff, and with a different number of PV modules and batteries are considered. The presented methodology allows the user to see the advantages and disadvantages of each system variant to choose an efficient and optimal microgrid concept according to its capabilities and criteria.

II. Determination of Basic Values in Grid-Connected Microgrids with a PV System

To design an on-grid photovoltaic system, it is necessary to know the potential of solar energy and ambient conditions. To determine the potential of solar energy, the measurement of horizontal irradiance and temperature should be performed at the location of the PV system. The total I_C irradiance reaching the PV module consists of three components: direct (I_{BC}), diffuse (I_{DC}) and reflected (I_{RC}) [26], as shown by the following relation:

$$I_C = I_{BC} + I_{DC} + I_{RC} \tag{1}$$

The direct irradiance I_{BC} reaching the PV collector is determined based on the direct irradiance I_{BH} on a horizontal surface [26]:

$$I_{BC} = I_{BH} R_B = I_{BH} \frac{\cos\theta}{\sin\beta} \tag{2}$$

where R_B is the slope factor, θ is the incident radiation angle on the collector and β is the altitude angle of the sun. Diffuse irradiance I_{DC} and reflected irradiance I_{RC} falling on a PV module with tilt angle Σ is determined according to the following relations [26]:

$$I_{DC} = I_{DH} \left(\frac{1+\cos\Sigma}{2} \right) \tag{3}$$

$$I_{RC} = \rho I_H \left(\frac{1-\cos\Sigma}{2} \right) \tag{4}$$

where I_H is the measured total horizontal irradiance, I_{DH} is the diffuse horizontal irradiance and ρ is the ground reflection coefficient.

The share of diffuse in the total horizontal radiation is determined based on Liu-Jordan's formula [26]. For its application, it is necessary to calculate the clearness index K_T, which is defined as the ratio of total horizontal insolation $\overline{I}_H$ at the measurement site on Earth to horizontal extraterrestrial insolation $\overline{I}_0$ on the atmosphere surface at latitude and longitude of the measurement site [26]:

$$K_T = \frac{\overline{I}_H}{\overline{I}_0} \tag{5}$$

The rated power of the PV module is declared by the manufacturer for standard test conditions. If N is the number of PV modules connected in series, then the installed power of the PV array is:

$$P_{DC(STC)} = NP_{DC(STC)1} \tag{6}$$

where $P_{\mathrm{DC(STC)1}}$ is the rated power of the PV module declared by the manufacturer for standard test conditions. Besides the irradiance on the PV modules, it is necessary to consider the influence of temperature on the efficiency of the PV modules to determine the power production of PV systems. The cell temperature of a PV module can be determined using the following formula [26]:

$$T_{PV} = T_{amb} + \left(\frac{NOCT - 20}{0.8}\right) I_C \tag{7}$$

where T_{PV} is the cell temperature of a PV module, T_{amb} is the ambient temperature, I_{C} is the solar irradiance on the surface of the module, *NOCT* is the cell temperature (°C) when the ambient temperature is 20 ^{0}C, solar irradiance is 0.8 kW/m^2, and wind speed is 1 m/s [26]. The influence of temperature on the reduction of the power of the PV module is calculated based on the temperature coefficient η_T defined for the rated power by the manufacturer of the PV module:

$$\eta_T = 1 + \alpha \cdot (T_{PV} - 25) \tag{8}$$

where α is the coefficient of change in the efficiency of the PV module due to temperature change concerning standard value of 25° C. The value of this coefficient is about 0.4%/°C.

The AC power delivered by the PV system to the distribution grid is less than the DC power under standard test conditions and is calculated as follows:

$$P_{\mathrm{PV}} = P_{\mathrm{DC(STC)}} \cdot \eta_{\mathrm{D}} \cdot \eta_M \cdot \eta_{\mathrm{T}} \cdot \eta_{\mathrm{inv}} \cdot \frac{I_{\mathrm{C}}}{1000} \tag{9}$$

where the coefficient η_{D} takes into account losses due to module contamination, the coefficient η_{M} takes into account losses due to mismatched modules, the coefficient η_{T} takes into account losses due to increasing module temperature above the standard value of 25 °C, and the coefficient η_{inv} represents the inverter efficiency.

The average power consumption diagram is obtained as the mean value of the power consumption of all households in a settlement, but such a diagram is not a reliable representation of the power consumption of one household. Compared to the power consumption diagram of one household, the average power consumption diagram is less variable because it is obtained based on a large number of households with different household appliances and different usage times. For that reason, the power consumption diagram of one household in this paper is modeled based on the rated powers of the household appliances and their usage time, adopting that power consumption fluctuates around the average power consumption diagram. To manage consumption, the consumption diagram of one household is divided into manageable and unmanageable parts.

Batteries are an integral part of many microgrids. The basic quantity for batteries that affects power management in the microgrid is the battery state of charge, which represents the battery level of charge over its rated capacity. In this paper, the case of grid-connected microgrid with a PV system and Li-ion batteries is also considered. The role of batteries is to accumulate electricity in periods of high production and low consumption, as well as deliver stored energy when needed. Batteries are practically always needed in off-grid PV systems. Batteries can also be used in on-grid PV systems to provide the user with the ability to store electricity in periods of high production and to use it in periods of low production (without buying energy from the grid), as well as to sell electricity when the price is favorable for the user. Despite all the above advantages, batteries are rarely used in on-grid systems, and the reason for this is the high cost of batteries, which increases investment. In addition, their lifespan is about 12 years, which means that new batteries must be purchased after the battery life expires.

III. Energy Flow Management in a Grid-Connected Microgrid by Applying a Fuzzy Logic Controller

A characteristic of many technical and economic systems is that they do not have sufficiently precise data at their inputs, so it is very common that they have at the disposal the data whose values contain a certain amount of uncertainty, i.e. they are not precise enough. During the decision-making or problem-solving process, the person responsible for making decisions most often relies on experience, intuition and subjective evaluation of individual parameters. The core of the fuzzy sets, that is, of the fuzzy logic, is inaccuracy or ambiguity. It can be freely said that significant technological progress has been achieved by solving the problems from different areas by applying the fuzzy set theory, i.e. fuzzy logic.

A fuzzy logic controller (FLC) is programmed to manage consumption in a grid-connected microgrid with a PV system and storage system, as shown in Fig. 1. The algorithm which uses the FLC controller manages the energy flow in the system and allows the charging and discharging of batteries as well as the energy exchange with the distribution grid, as shown in Fig. 2.

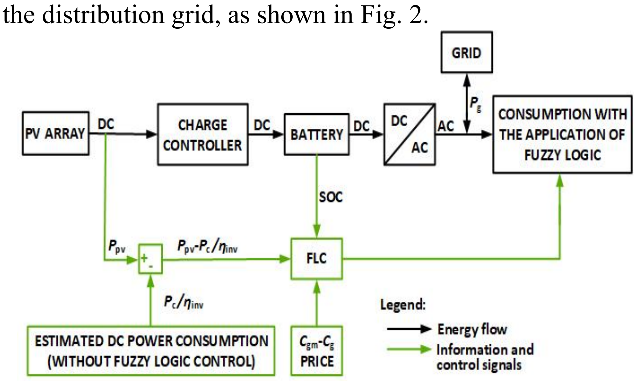

Figure 1. Consumption management system using FLC

The variables in Fig. 2 are: P_{cG1i} is the manageable power consumption, P_{cG2i} is the unmanageable power consumption, P_{ci} is the total power consumption, P_{pvi} is the total DC power production of the PV system, $P_{\mathrm{DC(STC)}}$ is the installed power of the PV array, I_{ci} is the solar irradiance to the solar collector, C_{g} is the price of electrical energy in the market, C_{gm} is the mean price of electrical energy in the market, W_{bi} is the actual energy stored in batteries, W_{bmax} is the maximum energy stored in batteries, η_{c} is the battery charging efficiency, η_{d} is the battery discharging efficiency, η_{inv} is the inverter efficiency, P_{mi} is the power exchange of the system with the distribution grid, and P_{bm} is the power exchange of the battery with the distribution grid. It can be seen from Fig. 2 that during the year the difference between the power production from RES and power consumption, as well as the SOC of the battery, are checked at any time t_i sampled with the step Δt.

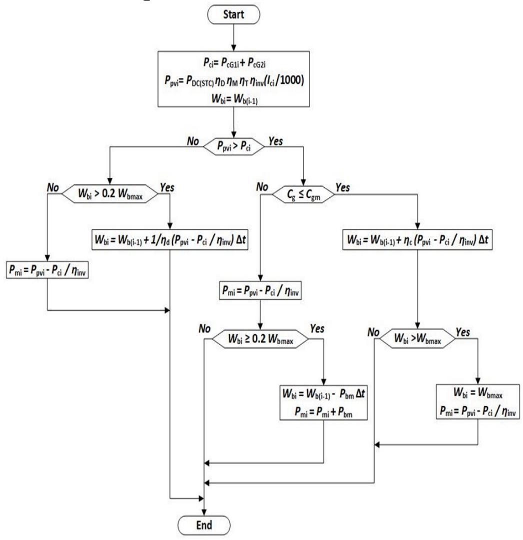

Figure 2. Algorithm for power flow management

IV. Grid-Connected Microgrid without Load Management

When forming the power consumption diagram, the data obtained by measuring consumption in a residential part of Belgrade, which has 1637 households, have been used. The average daily power consumption diagrams of one household P_{mean} are obtained by summing the corresponding 15-minute values from the daily power consumption diagrams of individual households and dividing by the number of households. However, such a daily diagram can not be considered as a credible power consumption diagram of one household. To have a completely credible daily power consumption diagram of one household, all the household appliances, their rated powers, and time of use in summer and winter seasons have been taken into account. These data are shown in Table I. The credible daily power consumption diagrams is formed to vary around the average daily power consumption diagram P_{mean}, taking into account the rated powers and time of use of appliances.

The data used in the process of sizing the PV array depend on 10-minute data on temperature and horizontal irradiance for the location of Belgrade whose latitudinal angle is L=45°. The PV modules are south-oriented at an optimal inclination angle of 34°, and the analyzed data cover a period of one year. In this paper, polycrystalline modules of rated power P_{max}=290 W with open-circuit voltage V_{oc}=39.33 V and short-circuit current I_{sc}=9.53 A are selected. A PV array containing 32 parallel-connected modules has been adopted. The installed power of the PV array is 9.28 kW. The rated power of the inverter is 10 kW, and the efficiency of the inverter is η_{inv}= 0.96. There have been adopted: the coefficient of efficiency: η_D = 0.96 which takes into account the contamination and aging of the modules, η_M=0.97 which takes into account the mismatch of the modules. The DC voltage of the system is U_s= 48 V. The used Li-ion battery has capacity A_{hb}=110 Ah, voltage U_b=24 V, and efficiency η_b= 0.95. The number of battery branches connected in parallel is n_{pb}= 6 and the number of batteries connected in series is n_{sb}= 2. The installed capacity of the battery system is 31.1 kWh, and the adopted price for this type of battery is 673.85 EUR.

A. Grid-connected Microgrid with Batteries and without a Feed-in Tariff

As first, the case of a grid-connected microgrid with batteries and without the feed-in tariff has been analyzed, i.e. the case when the production from the PV system is not subsidized. Fig. 3 (a) shows the power production P_{PV} from the PV system and the power consumption P_C for the period of one year (from 15 July 2013 to 14 July 2014). Fig. 3 (b) shows the power exchange P_g with the distribution grid for the same period of one year. The maximum power production from the PV system during the analyzed year is 7.63 kW. Fig. 4 shows the state of charge of the battery for the period of one year (from 15 July 2013 to 14 July 2014).

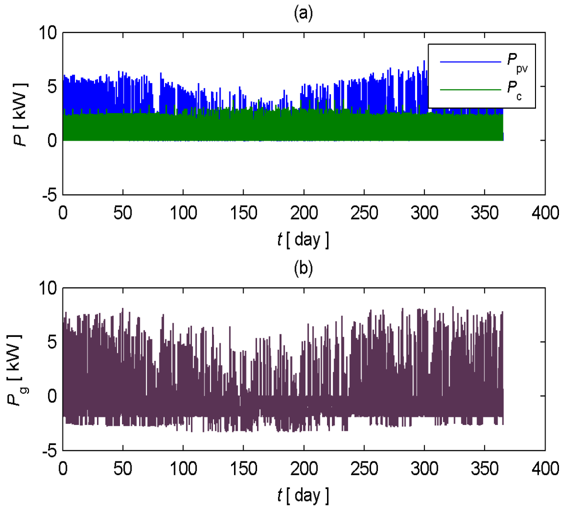

Figure 3. Grid-connected microgrid with batteries: (a) Annual power production P_{PV} from PV system and power consumption P_C; (b) Power exchange P_g with the distribution grid

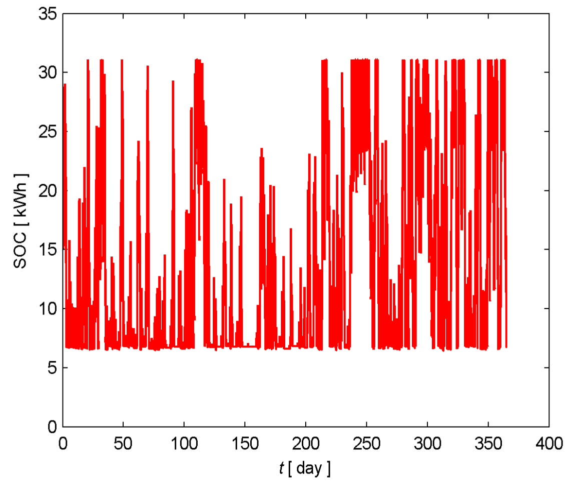

Figure 4. Grid-connected microgrid with batteries: Battery state of charge SOC

In the analyzed case, the grid-connected microgrid consisting of a PV system and energy storage system allows the users to meet their own needs for power consumption and achieve financial gain of 254.09 EUR/year in the energy exchange with the grid. The achieved financial gain has been calculated based on the power delivered to the distribution grid and the prices of electricity from the Hungarian Stock Exchange for the same period of one year (from 15 July 2013 to 14 July 2014). The user has large investments due to the price of batteries since the price of a used battery system based on the price of one battery is 8086.2 EUR. Since the production from the PV system is variable, in periods of small production and low battery SOC, it is necessary to take energy from the grid to supply appliences and preserve the user comfort.

B. Grid-connected Microgrid without Batteries and a Feed-in Tariff

Then the case of a grid-connected microgrid consisting of a PV system without an energy storage system has been analyzed. The user does not possess a feed-in tariff, and a financial gain of 234.02 EUR/year in the exchange of energy with the grid has been achieved. At the same time, the user has significantly less investment because the system does not contain batteries. If the production is higher than the consumption, the surplus electricity is sold to the grid at the electricity price on the stock exchange. In case when the production is lower than the consumption, the user will buy electricity from the grid at the electricity price on the stock exchange.

C. Grid-connected Microgrid without Batteries and with a Feed-in Tariff

The third analyzed case refers to a microgrid with a PV system without an energy storage system when the user possesses the feed-in tariff. The assumption is that the PV system must first supply the local consumption. In such conditions, the user has achieved the highest financial gain in the exchange of energy with the grid, of 1540.3 EUR/year. If the production is higher than the consumption, the surplus electricity is sold to the grid at the adopted price for the feed-in tariff of 206.6 EUR/MWh [27]. In case when the production is lower than the consumption, the user will buy electricity from the grid at the price of electricity on the stock exchange.

All three analyses have shown that the user has been provided with a continuous power supply while achieving a financial gain in the exchange of energy with the grid during the analyzed year. However, this does not mean that optimal consumption management has been achieved in a household. For the user to decide which microgrid is the most profitable one, it is not enough to make only the financial gain in the exchange of energy with the grid for one year. It is also important to perform an economic analysis that implies the calculation of investment costs, equipment maintenance, and replacement costs, as well as the calculation of profits during the lifetime of the analyzed system. After that, it is desirable to compare the calculated investment costs and the cost of equipment maintenance and replacement with the total profit over the lifetime and provide the user with an insight into the economic analysis of different microgrids.

V. GRID-CONNECTED MICROGRID WITH LOAD MANAGEMENT

To manage the consumption, consumption is divided into two groups: unmanageable consumption G_1 and manageable consumption G_2. The unmanageable consumption G_1 is the energy consumption of appliances that have to be supplied with electricity at any time. This means that the time of use cannot be postponed for a more favorable moment, for example when there is production from the PV system or when the price of electricity in the grid is lower. Manageable consumption G_2 includes the energy consumption G_{2a} of appliances whose switching time can be moved for a more favorable moment that is not during the night and the energy consumption G_{2b} of appliances whose switching time can be moved for any time of day (washing machine and water heater). The unmanageable consumption G_1 and the manageable consumptions G_{2a} and G_{2b} are shown in Table I.

TABLE I. APPLIANCE GROUPS

Group	Appliance	Rated power P_n [W]	Time of use in summer t_s[h/day]	Time of use in winter t_w [h/day]
G_1	Refrigerator	300	6	6
G_1	Lights (6 bulb)	6·80	2.78	4.19
G_1	TV active mode	80	2	4
G_1	TV standby mode	5.1	22	20
G_1	Antenna	3.5	2	4
G_1	Phone	4	24	24
G_1	PC active mode	125	1.5	1.5
G_1	PC standby mode	80	0.5	0.5
G_{2a}	Electric range	1000	2	2
G_{2b}	Water heater	1800	1.5	1.5
G_{2a}	Clothes iron	1000	1h/weekly	1h/weekly
G_{2a}	Air conditioner	1200	4	0
G_{2b}	Washing machine	1800	1.33h/weekly	1.33h/weekly
G_{2a}	Vacuum cleaner	750	30'/weekly	30'/weekly
G_{2a}	Microwave oven	700	0.17	0.17
G_{2a}	Coffeemaker	1200	0.17	0.17
G_{2a}	Toaster	800	0.17	0.17

Load management has been achieved by applying an FLC. The Mamdani type of inference was chosen, and the input data are the SOC of the battery, the differences between the output from the PV system (P_{pv}) and consumption (P_c), and the differences between the actual market price of electricity (C_g) and the average price of electricity on the market (C_{gm}). The input data for the FLC are shown in Figures 5-7 with the corresponding membership functions. The difference between the power production from the PV system and power consumption is shown in Fig. 5 and is represented by trapezoidal (Negative), triangular (Zero) and trapezoidal (Positive) membership functions. For the SOC, the membership functions of trapezoidal (Low), triangular (Medium) and trapezoidal (High) distribution have been assigned and are shown in Fig. 6. The difference between the current price of electricity during the year on the market C_g and the average price of electricity on the market C_{gm} are shown in Fig. 7 and are represented by trapezoidal (Negative), triangle (Positive) and trapezoidal (Very positive) membership function.

The output from the FLC is the probability of switching the unmanageable appliance group G_1 and the manageable appliance groups G_{2a} and G_{2b}.

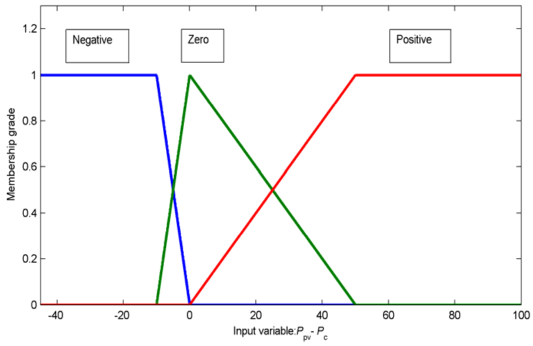

Figure 5. FLC input: Difference between power production from P_{PV} system and power consumption P_C

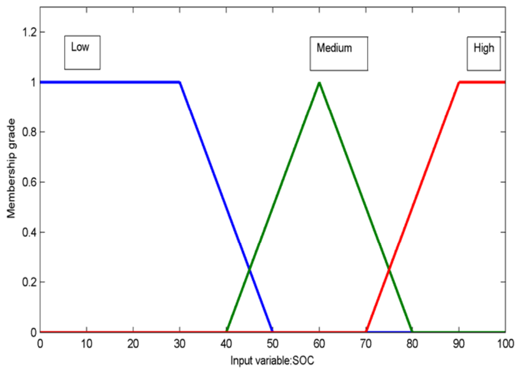

Figure 6. FLC input: Battery state of charge SOC

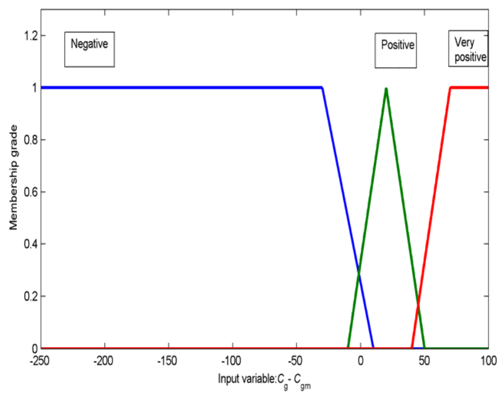

Figure 7. FLC input: The difference between the price of electricity on the market C_g and the mean value of electricity price during the year C_{gm}

The switching probabilities are represented by bell-shaped distribution functions denoted as Very low (Vl), Medium (Med) and Very high (Vh).

By using 54 if-then rules, smart consumption management is enabled while shifting the manageable consumption. In this way, optimal consumption management is achieved. Some of the fuzzy rules are shown in Table II.

Thanks to the application of the FLC, a shift in manageable consumption for a more favorable moment has been achieved. As the manageable consumption is divided into two groups, the time frames within which the consumption must be reimbursed taking into account the comfort of the users are defined accordingly. The consumption from G_{2a} must be reimbursed in the period from 07:00 to 00:00, and the consumption from G_{2b} can be reimbursed at any time of the day. In this way, optimal consumption management is achieved.

TABLE II. FLC RULES

No. of rules	Inputs and outputs from FLC				
	P_{PV}-P_C	SOC	C_g-C_{gm}	G_1	G_2
1.	Negative	Low	Negative	Vh	-
2.	Negative	Low	Very positive	Vh	-
3.	Zero	Medium	Positive	Vh	-
4.	Negative	High	Positive	Vh	
5.	Positive	High	Positive	Vh	-
6.	Negative	Low	Negative	Vh	Vl
7.	Negative	Low	Very positive	Vh	Vl
8.	Zero	Low	Negative	Vh	Med
9.	Negative	Medium	Negative	Vh	Vl
10.	Negative	Medium	Positive	Vh	Vl
11.	Negative	High	Positive	Vh	Vh
12.	Positive	High	Positive	Vh	Vh
13.	Positive	High	Very positive	Vh	Vh

A. Grid-connected Microgrid with Batteries and without a Feed-in Tariff

In a grid-connected microgrid with a PV system and battery energy storage, consumption management is achieved by using the FLC in the household. Fig. 8(a) shows the power consumption P_c before the application of the FLC and the new power consumption P_c^{new} after the application of the FLC. Fig. 8(b) shows the power production P_{pv} from the PV system and the power exchange P_g with the distribution grid. Fig. 9 shows the state of charge of the battery. The graphs shown in Fig. 8 and Fig. 9 cover a period of 7 days during the year.

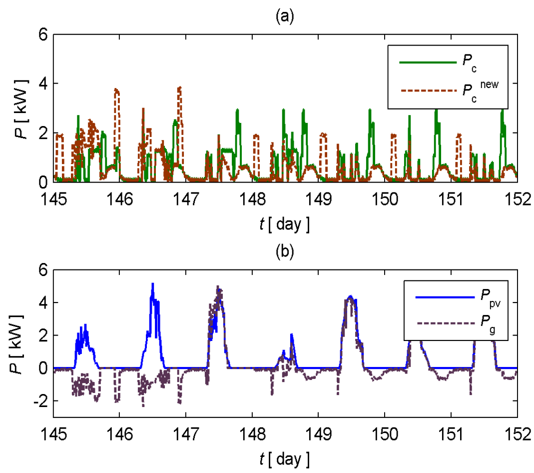

Figure 8. Grid-connected microgrid with PV system and batteries: (a) Power consumption P_C before application of FLC and power consumption P_C^{new} after application of FLC; (b) Power production P_{PV} from PV system and power exchange P_g with grid

From Fig. 8 and Fig. 9 it can be seen that the FLC manages the power supply of household consumption. The consumption is powered from the PV system, batteries, and distribution grid. Also, a shift in one part of consumption for a more favorable moment can be seen in Fig. 8. Thanks to the FLC, the number of batteries has been reduced from 12 to 6, which means that the number of battery branches connected in parallel is now n_{pb}=3, and the number of batteries connected in series is n_{sb}=2.

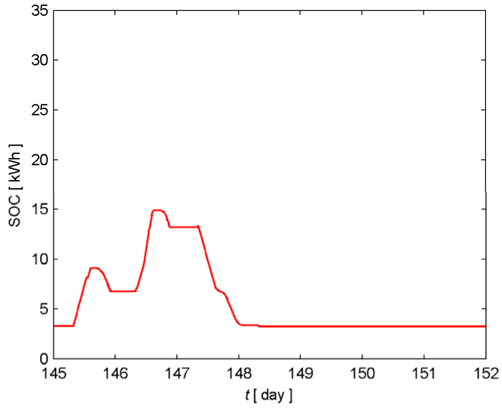

Figure 9. Grid-connected microgrid with PV system and batteries: Battery state of charge SOC

Fig. 10(a) shows the power production P_{pv} from the PV system and the power exchange P_g with the distribution grid. Fig. 10(b) shows the diagram of the electricity price C_g on the market and the mean value of the electricity price C_{gm} during the analyzed period of 7 days.

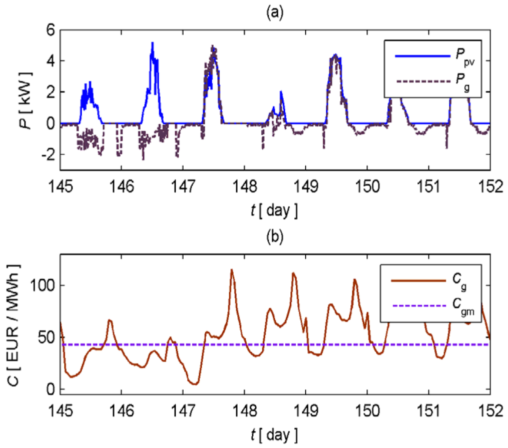

Figure 10. Grid-connected microgrid with PV system and batteries: (a) Power production P_{PV} from PV system and power exchange P_g with distribution grid; (b) Electricity price C_g and mean value of electricity price C_{gm}

Fig. 10(b) shows the time intervals in which energy is sold (when $C_g > C_{gm}$) or purchased (when $C_g < C_{gm}$) from the distribution grid depending on the availability of energy from the PV system and batteries, and the price of electricity in the grid. If the owner of the PV system does not have benefits that include a feed-in tariff, he will try to supply own consumption first and then to sell the excess energy to the distribution grid when the electricity price on the market is higher than average. The boundary between the cheap and expensive electricity prices is adopted and represented by the average value of electricity price C_{gm}. The user will buy energy from the distribution grid when it is cheap (lower than the average value of the price of electricity C_{gm}) and sell it to the grid when it is expensive (higher than the average value of the electricity price C_{gm}). The user realizes this exchange of energy with the distribution grid by shifting his consumption, and the benefit of that is additional financial gain.

With the application of the FLC and electricity flow management algorithm, it is possible to supply consumers with electricity, achieving a financial gain of 285.14 EUR/year in the energy exchange with the grid. This analysis has been done under the assumption that the user does not have a feed-in tariff. It should be borne in mind that this is an annual financial gain and that, based on it, the user can calculate whether he will operate with profit or loss during the lifetime of the entire system, which amounts to 24 years.

A more detailed analysis of the mentioned variants of the microgrid has been performed by varying the number of batteries and PV modules in the system. The case with a fixed number of PV modules (n=32) and a different number of batteries has been analyzed. The number of batteries analyzed in this case is n_b=2, 6, 10, and 14. The investment costs of the PV system of 1 EUR/W were adopted, and the maintenance costs are 3% of the investments in the PV system. The price of one battery of 673.85 EUR has been adopted. Fig. 11 shows a diagram of the total price C_s of the PV system and batteries, the achieved profit D_s during the lifetime of 24 years without the application of the FLC, and the achieved profit D_{sFLC} with the application of the FLC, depending on the number of batteries n_b.

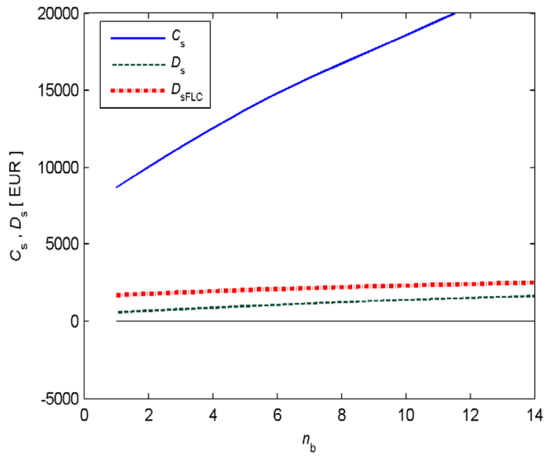

Figure 11. Total price C_s of PV systems and batteries, achieved profit D_S during the lifetime without application of FLC and achieved profit D_{sFLC} with application of FLC for case of PV system with different number of batteries and without application of feed-in tariff

Based on the displayed comparative diagrams, one concludes that such a system is never profitable because the price of the total system C_s is significantly higher than the achieved profit due to increasing costs for the price of batteries whose lifetime is 12 years. This means that it is necessary to buy batteries twice during the considered system lifetime of 24 years. According to the battery manufacturer's specifications, more than 2000 cycles of charging and discharging are allowed during battery lifetime. For the case without the application of the FLC, the number of cycles is 1281. With the application of the FLC, the number of cycles is reduced by 62 and amounts to 1219 over 12 years. It can be concluded that the FLC has a favorable effect on reducing the number of charge and discharge cycles and thus has a positive effect on the battery lifetime. However, such a system is still unprofitable for the entire lifetime of the system due to the high cost of the PV system, batteries, and system maintenance.

B. Grid-connected Microgrids without Batteries and a Feed-in Tariff

A system consisting of a PV system without batteries and a feed-in tariff has also been considered. The price C_s of the

PV system and the achieved profit D_s have been analyzed during the entire lifetime of 24 years, depending on the number of PV modules n. Fig. 12 shows the price C_s of the PV system, the achieved profit D_s during the lifetime without the application of the FLC, as well as the achieved profit D_{sFLC} with the application of the FLC. The cost C_s and profit D_s for a period of 24 years are discounted to the initial year. It can be seen from Fig. 12 that such a system is never profitable for the user regardless of the number of PV modules n. With the increase in the number of PV modules the investment costs C_s increase faster than the achieved profit of the system D_s. Also, it can be concluded that the profit in the exchange of energy with the grid has a negative value for a relatively small number of PV modules.

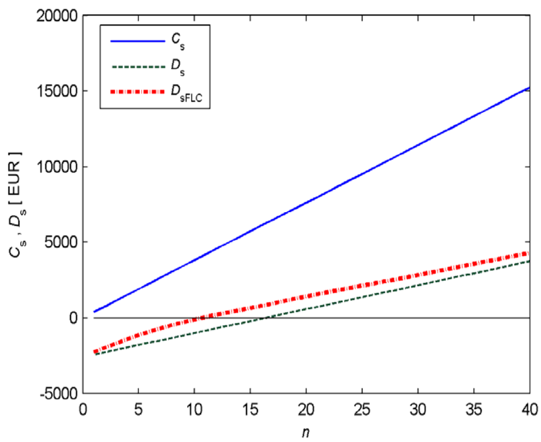

Figure 12. Price C_s of PV system, achieved profit D_s during the lifetime without application of FLC and achieved profit D_{sFLC} with application of FLC for case of PV system without batteries and without application of a feed-in tariff, depending on a number of PV modules n

There has also been analyzed an energy flow management algorithm that uses the FLC in a grid-connected microgrid with n=32 PV modules but without batteries. Fig. 13(a) shows the power consumption P_c before the application of the FLC and the new power consumption P_{cnew} after the application of the FLC. Fig. 13(b) shows the power production P_{pv} from the PV system and the power exchange P_g with the distribution grid.

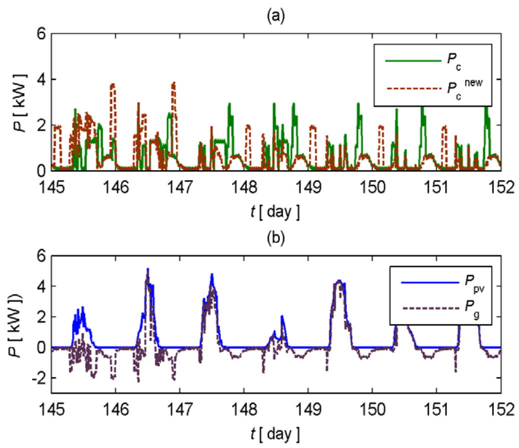

Figure 13. Grid-connected microgrid with PV system without batteries: (a) Power consumption P_C before application of FLC and power production P_C^{new} after application of FLC; (b) Power production P_{PV} from PV system, and power exchange P_g with distribution grid

It can be seen from Fig. 13 that the consumption is supplied at a given moment or is shifted to a more favorable moment within the defined range. There is a higher takeover of electricity from the distribution grid due to the lack of an electricity storage system.

Thanks to the application of the FLC to manage consumption, the system has become more effective. A financial gain of 292.78 EUR/year in the energy exchange with the grid has been achieved. However, based on Fig. 12, it can be seen that the system is still unprofitable during its lifetime regardless of the number of PV modules n, since there is no intersection of the curve of the (true) price C_s of the system and the profit D_{sFLC} in the energy exchange with the grid

C. Grid-connected Microgrid without Batteries and with a Feed-in Tariff

The next analysis has been performed for a grid-connected microgrid with a PV system without batteries and with a feed-in tariff for 12 years. This means that the user has a feed-in tariff during the first 12 years of the microgrid's lifetime of 24 years. The price C_s of the PV system, the achieved profit D_s without the use of the FLC, and the achieved profit D_{sFLC} with the use of FLC, during a lifetime of 24 years, have been analyzed depending on the number of PV modules to find a cost-effective PV system for the use, as shown in Fig. 14.

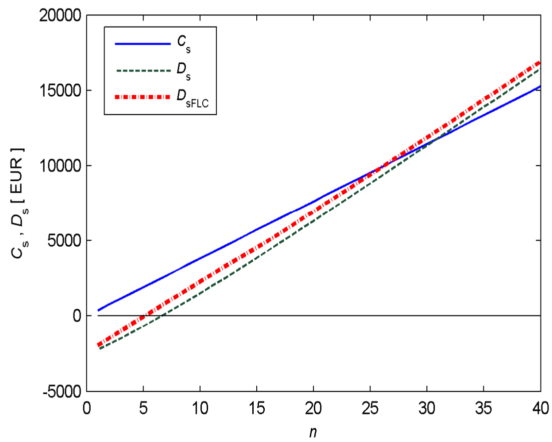

Figure 14. Price C_s of PV system, achieved profit D_s during the lifetime without application of FLC and achieved profit D_{sFLC} with application of FLC for case of PV system without batteries and with application of feed-in tariff as a function of number of PV modules n

It is noticed that the profit increases faster than system cost with the increase of the number of PV modules. The system without the application of the FLC is not profitable when the number of modules is lower than 31. It means that such a system becomes cost-effective when the number of PV modules is higher than or equal to 31. However, it can be seen from Fig. 14 that the microgrid is always more cost-effective with the application of the FLC and consumption management algorithm. From the intersection of the curve C_s and D_{sFLC}, it can be seen that the microgrid is profitable when the number of PV modules is higher than or equal to 27. Thanks to FLC, the number of PV modules n=32 in the considered example is well-chosen, while the PV system has a significant share in supplying the load during the year (27.04%).

For the same microgrid, if the user is considered to have a feed-in tariff, it is possible to achieve a financial gain of 1593.1 EUR/year in the energy exchange with the grid. Fig.

15(a) shows the power production P_{pv} from the PV system and the power of exchange P_g with the distribution grid. Fig. 15(b) shows the diagram of the price C_g of electricity on the market, the average electricity price C_{gm}, the price C_s based on which electricity is sold/bought from the grid, and the price C_{ft} which implies the presence of the feed-in tariff during the analyzed period. If the production from the PV system is higher than the consumption, the excess energy is sold to the grid at the price of the feed-in tariff, which can be seen in the diagram when C_s reaches the value of the price C_{ft}. If the production from the PV system is lower than the consumption, then the energy is bought from the grid at a price equal to the price of electricity on the market, which is seen in the diagram when C_s reaches the value of the price C_g. Due to the consumption management, the manageable appliances (appliances from groups G_{2a} and G_{2b}) switch on when the price of electricity in the grid is lower, to place surplus energy in the grid later when the grid needs it most. For that reason, it is necessary to monitor at all times whether the energy in the grid is cheap or expensive.

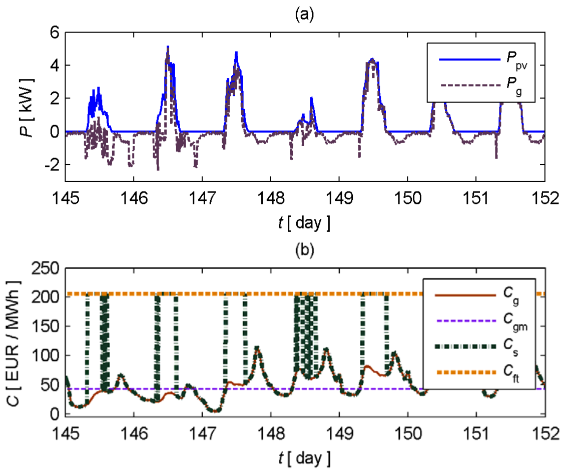

Figure 15. Grid-connected microgrid with PV system without batteries: (a) Power production P_{PV} from PV system and power exchange P_g with distribution grid; (b) Electricity price C_g, mean value C_{gm} of electricity price, sale/purchase electricity price C_s and price C_{ft} that includes feed-in tariff

VI. Conclusion

The aim of this paper is to compare different variants of a microgrid with a PV system for three different cases: with batteries and without a feed-in tariff, without batteries and a feed-in tariff, and without batteries and with a feed-in tariff. The first two microgrid concepts do not give satisfactory results to the user. It is important for the user to have an electricity supply without compromising comfort and to achieve profit during the lifetime of the microgrid. From that point of view, the highest financial gain is achieved in a grid-connected microgrid with a PV system, without batteries, and with a feed-in tariff. Besides the comparative analysis of different microgrid concepts, this paper also performs the consumption management by using the FLC and algorithm for power flow management, which has resulted in higher financial profits. The economic analysis has shown that a grid-connected microgrid with a PV system, with or without batteries, and without feed-in tariff is not cost-effective during its lifetime, even with the application of the FLC. The reasons for this are the high cost of investment and replacement of batteries over a lifetime and the lack of subsidies (feed-in tariffs). Only a grid-connected microgrid with a PV system without batteries and with a feed-in tariff enables financial gain during its lifetime. With the application of FLC for consumption management, the user can achieve higher profit or make the system cost-effective with fewer PV modules. Due to the energy flow optimization, the microgrid with the FLC and a power flow algorithm has an advantage. The application of such techniques, together with the advancement of PV technology and the growing demand for PV systems, will contribute to making micro-grids cost-effective and widely applicable.

Acknowledgment

The authors are grateful to the Ministry of Science and Technological Development of Serbia for the support of this work through technological project III42009 and TR-33037.

References

[1] A. Hirsh, Y. Parag, J. Guerrero, “Microgrids: A review of technologies, key drivers, and outstanding issues,” Renewable and Sustainable Energy Reviews, vol. 90, pp. 402-411, 2018. doi:10.1016/j.rser.2018.03.040

[2] Y. Zahraoui, I. Alhamrouni, S. Mekhilef, M. R. Basir Khan, M. Seyedmahmoudian, A. Stojcevski, B. Horan, “Energy management system in microgrids: A comprehensive review,” Sustainability, vol. 13, no. 19, pp. 10492, 2021. doi:10.3390/su131910492

[3] S. Jamal, N. M. L. Tan, J. Pasupuleti, “A review of energy management and power management systems for microgrid and nanogrid applications,” Sustainability, vol. 13, no. 18, pp. 10331, 2021. doi:10.3390/su131810331

[4] M. F. Zia, E. Elbouchikhib, M. Benbouzid, “Microgrids energy management systems: A critical review on methods, solutions, and prospects,” Applied Energy, vol. 222, pp. 1033-1055, 2018. doi:10.1016/j.apenergy.2018.04.103

[5] B. Jyoti Saharia, H. Brahma, N. Sarmah, “A review of algorithms for control and optimization for energy management of hybrid renewable energy systems,” Journal of Renewable and Sustainable Energy, vol. 10, no. 5, pp. 053502, 2018. doi:10.1063/1.5032146

[6] A. Borni, T. Abdelkrim, L. Zaghba, A. Bouchakour, A. Lakhdari, L. Zarour, “Fuzzy logic, PSO based fuzzy logic algorithm and current controls comparative for grid-connected hybrid system,” AIP Conference Proceedings, vol. 1814, no. 1, pp. 020006, 2017. doi:10.1063/1.4976225

[7] K. S. Ei-Bidairi, H. D. Nguyen, S. D. G. Jayasinghe, T. S. Mahmoud, “Multiobjective intelligent energy management optimization for grid-connected microgrids,” 2018 IEEE International Conference on Environment and Electrical Engineering and 2018 IEEE Industrial and Commercial Power Systems Europe (EEEIC / I&CPS Europe), IEEE, pp 1–6, 2018. doi:10.1109/EEEIC.2018.8493751

[8] A. J. Aristizábal, D. H. Ospina, M. Castañeda, S. Zapata, E. Banguero, “Fuzzy logic energy management for a microgrid with storage battery,” International Journal of Ambient Energy, vol. 41, no. 10, pp. 1183-1191, 2020. doi:10.1080/01430750.2018.1507931

[9] S. Das, A. K. Akella, “Power flow control of PV-wind-battery hybrid renewable energy systems for stand-alone application,” International Journal of Renewable Energy Research, vol. 8, no. 1, pp. 36-43, 2018. doi:10.20508/ijrer.v8i1.6534.q7278

[10] D. Arcos-Aviles, J. Pascual, L. Marroyo, P. Sanchis, F. Guinjoan, “Fuzzy logic-based energy management system design for residential grid-connected microgrids,” IEEE Transactions on Smart Grid, vol. 9, no. 2, pp. 530-543, 2018. doi:10.1109/TSG.2016.2555245

[11] U. Datta, J. Shi, A. Kalam, “Primary frequency control of a microgrid with integrated dynamic sectional droop and fuzzy based pitch angle control,” International Journal of Electrical Power & Energy Systems, vol. 111, pp. 248–259, 2019. doi:10.1016/j.ijepes.2019.04.001

[12] G. Saveen, P. Prudhvi Raju, D. V. Manikanta, M. Satya Praveen, “Design and implementation of energy management system with fuzzy control for multiple microgrid,” 2018 2nd International Conference on Inventive Systems and Control (ICISC), IEEE, pp. 1239–1244, 2018. doi:10.1109/ICISC.2018.8399003

[13] P. Tenti, H. K. Morales Paredes, P. Mattavelli, “Conservative power theory, a framework to approach control and accountability issues in smart microgrids,” IEEE Transactions on Power Electronics, vol. 26, no. 3, pp. 664-673, 2011. doi:10.1109/TPEL.2010.2093153

[14] Y. Zhou, “The optimal home energy management strategy in smart grid,” Journal of Renewable and Sustainable Energy, vol. 8, no. 4, pp. 045101, 2016. doi:10.1063/1.4955045

[15] E. D. Santis, A. Rizzi, A. Sadeghian, “Hierarchical genetic optimization of a fuzzy logic system for energy flows management in microgrids,” Applied Soft Computing, vol. 60, pp. 135-149, 2017. doi:10.1016/j.asoc.2017.05.059

[16] J. P. Fossati, A. Galarza, A. Martín-Villate, J. M. Echeverría, L. Fontán, “Optimal scheduling of a microgrid with a fuzzy logic controlled storage system,” International Journal of Electrical Power & Energy Systems, vol.68, pp. 61-70, 2015. doi:10.1016/j.ijepes.2014.12.032

[17] A. Chaouachi, R. M. Kamel, R. Andoulsi, K. Nagasaka, “Multiobjective intelligent energy management for a microgrid,” IEEE Transactions on Industrial Electronics, vol. 60, no. 4, pp. 1688–1699, 2013. doi:10.1109/TIE.2012.2188873

[18] D. Arcos-Avilesa, J. Pascualb, F. Guinjoanc, L. Marroyob, P. Sanchisb, M. P. Mariettac, “Low complexity energy management strategy for grid profile smoothing of a residential grid-connected microgrid using generation and demand forecasting,” Applied Energy, vol. 205, pp. 69-84, 2017. doi:10.1016/j.apenergy.2017.07.123

[19] T. T. Teo, T. Logenthiran, W. L. Woo, K. Abidi, T. John, N. S. Wade, D. M. Greenwood, C. Patsios, P. C. Taylor, “Optimization of fuzzy energy-management system for grid-connected microgrid using NSGA-II,” IEEE Transactions on Cybernetics, vol. 51, no. 11, pp. 5375 -5386, 2021. doi:10.1109/TCYB.2020.3031109

[20] S. Leonori, E. De Santis, A. Rizzi, F. M. F. Mascioli, “Optimization of a microgrid energy management system based on a Fuzzy Logic Controller,” IECON 2016 - 42nd Annual Conference of the IEEE Industrial Electronics Society, IEEE, pp 6615–6620, 2016. doi:10.1109/IECON.2016.7793965

[21] S. Chakraborty, T. Ito, T. Senjyu, A. Yousuf Saber, “Intelligent economic operation of smart-grid facilitating fuzzy advanced quantum evolutionary method,” IEEE Transactions on Sustainable Energy, vol. 4, no. 4, pp. 905-916, 2013. doi:10.1109/TSTE.2013.2256377

[22] M. Khalida, R. P. Aguilerab, A. V. Savkinc, V. G. Agelidisd, “On maximizing profit of wind-battery supported power station based on wind power and energy price forecasting,” Applied Energy, vol. 211, pp. 764-773, 2018. doi:10.1016/j.apenergy.2017.11.061

[23] L. Zec, J. Mikulović, “Load management in an off-grid hybrid PV–Wind–Battery system using the power flow control algorithm and fuzzy logic controller,” Electrical Engineering, vol.104, no. 4, pp. 2185-2195, 2022. doi:10.1007/s00202-021-01463-7

[24] W. Zhuo, “Microgrid energy management strategy with battery energy storage system and approximate dynamic programming,” 2018 37th Chinese Control Conference (CCC), IEEE, pp.7581-7587, 2018. doi:10.23919/ChiCC.2018.8482602

[25] L. Xiong, P. Li, Z. Wang, J. Wang, “Multi-agent based multi objective renewable energy management for diversified community power consumers,” Applied Energy, vol. 259, pp. 114140, 2020. doi:10.1016/j.apenergy.2019.114140

[26] G. M. Masters, “Renewable and efficient electric power systems,” pp. 410-527, Stanford University, 2004

[27] Decree on incentive measures for subsidized electricity producers, Official Gazette of the Republic of Serbia, no. 8/2013, 25th January 2013